Nanoscale

COMMUNICATION

View Article Online
View Journal | View Issue

Blue emitting undecaplatinum clusters†

Cite this: *Nanoscale*, 2014, **6**, 8561

Indranath Chakraborty, Radha Gobinda Bhuin, Shridevi Bhat and T. Pradeep*

Received 21st May 2014
Accepted 27th May 2014

DOI: 10.1039/c4nr02778g

www.rsc.org/nanoscale

A blue luminescent 11-atom platinum cluster showing step-like optical features and the absence of plasmon absorption was synthesized. The cluster was purified using high performance liquid chromatography (HPLC). Electrospray ionization (ESI) and matrix assisted laser desorption ionization (MALDI) mass spectrometry (MS) suggest a composition, $Pt_{11}(BBS)_8$, which was confirmed by a range of other experimental tools. The cluster is highly stable and compatible with many organic solvents.

Noble metal quantum clusters (QCs), also referred to as monolayer protected clusters, artificial atoms, and nanomolecules belong to a fascinating area of current research owing to their unique optical and photochemical properties.[1–6] The smaller size (less than 2 nm), high quantum confinement and the absence of surface plasmon resonance make these materials molecule-like. Due to the enhanced optical and photochemical properties, they have been used in many applications such as bio-labeling,[7,8] drug delivery,[9] cancer cell imaging[10] and many others.[11,12] Among the noble metals, gold has been explored significantly. Crystal structures of clusters such as Au_{23},[13] Au_{25},[6,14] Au_{36},[15] Au_{38},[16,17] and Au_{102}[18] have been reported. Unlike in the case of gold, a very few reports namely $Ag_{7,8}$,[19] Ag_9,[20] Ag_{32},[21] Ag_{44}[22,23] and Ag_{152}[24] exist for silver clusters with detailed characterization. Crystal structures of a few of the silver analogues of QCs are available recently.[25–28] There are a very few reports on luminescent Pt clusters[29–33] which are either polymer (pentaerythritol tetrakis 3-mercaptopropionate–polyvinylacetate, PTMP–PVAc)-protected,[30] dendrimer-protected,[29] or glutathione (GSH)-protected.[31] However, improved characterization, especially detailed mass spectrometric studies are needed to know each of these systems in much more detail, particularly their precise compositions as many atomically precise clusters have still not been crystallized.[18–22,34] Besides synthesizing new clusters with versatile methods, accurate and reproducible separation would enable improved characterization of these materials. As Pt has high catalytic activity,[35] discovery of such clusters can enhance the field tremendously.

In this work, we report the synthesis of a blue emitting monolayer protected atomically precise Pt_{11} cluster. Detailed characterization of the chromatographically-isolated cluster was done by electrospray ionization mass spectrometry (ESI MS) and matrix assisted laser desorption ionization mass spectrometry (MALDI MS) in order to identify its precise composition.

The synthesis of the Pt cluster follows a solid state route[20] which was originally developed for Ag_9 clusters protected with mercaptosuccinic acid (MSA). In this method, H_2PtCl_6(s) was ground with 4-(*tert*-butyl)benzyl mercaptan (BBSH) (l) at 1 : 10 molar ratio with a mortar and pestle. Then 40 mg of $NaBH_4$(s) was added and grinding was continued for 2 minutes to complete the reaction. Immediate extraction of excess thiol in the reaction mixture with 5 mL of ethanol and subsequent dissolution of the residue in toluene makes the crude cluster (details are given in ESI1†). This was further analyzed with high performance liquid chromatography (HPLC) and the Pt_{11} cluster was isolated as a deep yellow solution and was used for further characterization.

The UV/Vis of the crude cluster shows (Fig. 1A) two broad bands at 3.13 eV (395 nm) and 3.98 eV (310 nm) with a threshold of absorption at 1.06 eV. The latter one may correspond to the interband (sp–d) transition from metal to thiolate and the former one may be due to the intraband (sp–sp) transition.[31] The step-like feature confirms the formation of molecule-like species. It is important to note that unlike in the case of gold and silver nanoparticles, platinum does not exhibit any surface plasmon absorption in the visible region.[29] None of the known clusters of platinum show distinct features.[29–33]

DST Unit of Nanoscience (DST UNS) and Thematic Unit of Excellence (TUE), Department of Chemistry, Indian Institute of Technology Madras, Chennai 600 036, India. E-mail: pradeep@iitm.ac.in; Fax: +91-44-2257 0545

† Electronic supplementary information (ESI) available: Details of experimental procedures, instrumentation, chromatogram of the crude cluster; SEM/EDAX, DLS, PXRD, TEM, FT-IR, and XPS of the isolated Pt_{11} cluster; UV/Vis, MALDI MS and SEM/EDAX of isolated 2 and 3; and ^{195}Pt NMR of the K_2PtCl_6 standard. See DOI: 10.1039/c4nr02778g

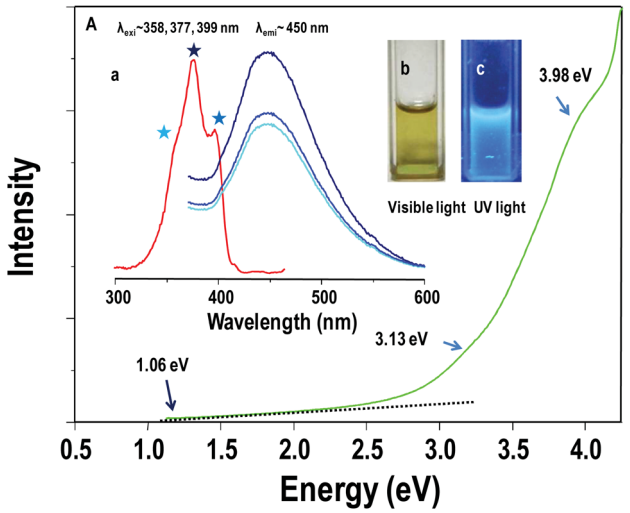

Fig. 1 UV/Vis spectrum of the as-synthesized Pt cluster plotted in terms of energy. Jacobian-corrected intensities are plotted. The spectrum shows two humps near 3.13 and 3.98 eV. Inset 'a' shows the luminescence spectral data. Three emission spectra, collected at the maxima shown by the excitation spectrum are shown. The excitation spectrum was collected for emission at 450 nm, which is the maximum exhibited in all the emission spectra. Insets 'b' and 'c' are the photographs under visible and UV light, respectively.

The cluster shows blue luminescence (Fig. 1c) under UV light with a quantum yield of 3×10^{-3} (details of the QY calculation is given in the ESI†) which is quite low compared to the dendrimer encapsulated blue emitting cluster, proposed to be $Pt_5(MAA)_8$ (MAA = mercaptoacetic acid), reported by Tanaka *et al.*[29] Three excitation features were observed for our cluster at 358, 275 and 399 nm (Fig. 1a). All of them give rise to the same emission feature at 450 nm.

The as-synthesized crude cluster was run through a HPLC system with a normal phase column (Fig. S2A, ESI†). Toluene was used as the mobile phase with 1 mL min^{-1} flow rate under isocratic conditions and a UV/Vis detector was set for this experiment. Three peaks were observed (Fig. S2A, ESI†), among them, only the first one (marked as 1), eluted at 6.3 min retention time, shows the UV/Vis pattern nearly identical to the spectrum of the crude cluster (Fig. S2B, ESI†). The blue luminescence and emission features (data not shown) were also identical. The other two peaks (marked 2 and 3) did not show any UV/Vis features (Fig. S3, ESI†). Individual components were collected and used for further characterization. The last two components did not show any MALDI MS features (Fig. S3, ESI†), which are likely to be decomposed thiolates. SEM/EDAX (Fig. S4, ESI†) was used to know the elemental ratio in these samples. Both of them have the same atomic ratio of Pt and S (1 : 4) and they form needle-like microcrystals which suggest the possibility of PtL_4 type thiolates. As we are interested in the cluster with molecular features we progressed further only with this species.

The purified cluster eluted at 6.3 min in HPLC was subjected to MALDI MS studies. Here, *trans*-2-[3-(4-*tert*-butylphenyl)-2-methyl-2-propenylidene]malononitrile (DCTB) was used as the matrix as it is known to give a better resolved mass spectrum.[24,34,36,37] The spectrum shows (Fig. 2) a prominent peak centered at m/z 3600 ± 50. Compared to the $Au_{25}(PET)_{18}$ cluster, the FWHM of the Pt cluster is broad. This is mainly because of its isotopes (^{192}Pt, ^{194}Pt, ^{195}Pt, ^{196}Pt, ^{198}Pt) whereas gold has only one (^{197}Au). So, in comparison to gold the FWHM of the Pt cluster will be significantly large. However, it is obvious that the observed peak width is not only due to the isotope width alone, there are other factors such as fragmentation. Laser intensity dependence of the spectrum was studied (Fig. S5A, ESI†). From our previous study,[24] we know that the increase in laser power gives fragmentation which may be used to understand the structure of the monolayer protected cluster. Increase in the laser power (from 1840 to 2640, in instrument units) results in an additional broad hump around m/z 7200 ± 100 and a sharp peak at ~m/z 2150 (Fig. S5A, ESI†). Further increase in the laser power does not show any change in the spectrum. The broad shoulder at m/z 7200 may be due to the dimer generated at a higher laser power and the sharp peak at m/z 2150 may correspond to the metallic core or the fragmented species. The cluster species may also contain weakly bound ligands which may have desorbed during desorption-ionization. As the mass spectra of platinum clusters are not available in the literature, we compare the MALDI MS data with those of the Ag_{44} system (Fig. S5B, ESI†) which is also broad. The data presented suggest that the number of ligands present in the cluster may be 8 ((3600−2150)/179 = 8.10) and the core may contain 11 (2150/196 = 10.96) Pt atoms.

ESI MS analysis was carried out to know the composition precisely. For this experiment, an external ionizing agent, caesium acetate (CsOAc) was used, as the ligand is completely non-polar. The toluene–methanol mixture (1 : 1) was used as a solvent and the spectrum was collected in the positive mode.

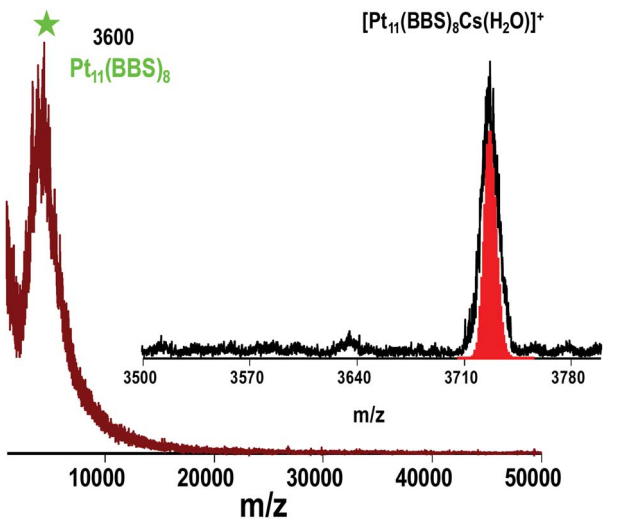

Fig. 2 MALDI MS data of the purified cluster. Molecular peak at m/z 3600 was observed at threshold laser power. The inset shows the ESI mass spectrum of the purified cluster. CsOAc was used as an ionization enhancer. The red sticks show the calculated spectra for the corresponding composition.

The ESI MS shows a very clean spectrum with a peak at *m*/*z* 3730 along with some fragmented peaks in the lower mass region (Fig. 2 and S6, ESI†). Fragmentation does occur under electrospray conditions, which has been observed for many clusters.[23,24] This is mainly because of the high stability of the specific fragments under the ionizing conditions. The fragments form even under softer conditions. Spectra under various conditions are plotted in Fig. S7, ESI.† The peak at *m*/*z* 3730 was assigned to $[Pt_{11}(BBS)_8Cs(H_2O)]^+$. The attachment of Cs and H_2O to a cluster may be surprising, but similar attachments have been observed in clusters.[35,37,38] Attachment of Cs^+ is common to neutral species in secondary ion mass spectrometry (SIMS).[39] The experimental spectrum matches exactly with the calculated spectrum (compared in the inset of Fig. 2). It is important to note that the corresponding gold analogue with a composition of $Au_{11}(PPh_3)_8Cl_3$ is reported, although these two may have completely different structures.[40,41] No chlorine incorporation was seen in EDAX or in other measurements. In the lower mass region, the intense peak at *m*/*z* 1791 is due to a stable fragment of composition, $Pt_3(BBS)_6Cs$ (Fig. S6, ESI†). The isotope distribution is matching with the corresponding calculated spectrum. Next to the stable fragment, a less intense peak at *m*/*z* 1836 is assigned to $Pt_3(BBS)_7$, again supported by the calculated spectrum. We did not observe any multiply charged species in the spectrum. MS/MS was also tried but nothing significant came out from this analysis.

The TEM image shows the presence of clusters and they appear as tiny dots with an average diameter of 0.7 nm (Fig. S8, ESI†). The narrow size distribution also suggests the monodispersity of the clusters. Another important aspect is that the clusters are sensitive to the electron beam. With longer time irradiation, they aggregate themselves to form bigger particles. Dynamic light scattering (DLS) confirms the monodispersity of the product. A very narrow size distribution curve was seen with an average particle size of 1.5 nm (Fig. S9, ESI†). We note that the hydrodynamic diameter of the cluster includes the ligand shell as well. The SEM/EDAX (Fig. S10, ESI†) also supports the composition where the Pt : S ratio was 1 : 0.737 (expected ratio is 1 : 0.727). The IR spectra of the Pt_{11} cluster and BBSH thiol are given in Fig. S11, ESI.† The absence of S–H stretching at 2587 cm^{-1} suggests the binding mode of thiol as thiolate (RS^-). Thermogravimetric analysis (Fig. 3A) showed a 39.91% mass loss (calculated, 40.02%) which further supports the composition. X-ray photoelectron spectroscopy (XPS) was carried out to confirm the valence state of the elements. The survey spectrum (Fig. S12, ESI†) shows the presence of expected elements such as C 1s, Pt 3d, Pt 4f, Pt 4p, Pt 4s and S 2p. The Pt : S ratio was found as 1 : 0.729. The expanded spectrum in the Pt 4f region shows (Fig. 3B) two peaks at 71.9 eV and 75.3 eV (corresponding to $4f_{7/2}$ and $4f_{5/2}$, respectively), corresponding to the zero valent state of Pt.[31] C and S show peaks at the expected positions (Fig. S13, ESI†). The S 2p peak at 162.4 eV confirms the binding of thiol in the thiolate form. Powder X-ray diffraction (PXRD) analysis (Fig. S14, ESI†) was carried out for the cluster in the 2θ range of 10–90°. The pattern shows broad diffraction peaks centered around 39°, 45° and 66°. Nanoclusters having molecule-like properties are small to contain a periodic lattice in them and so they do not show sharp peaks as seen for noble metal nanoparticles.

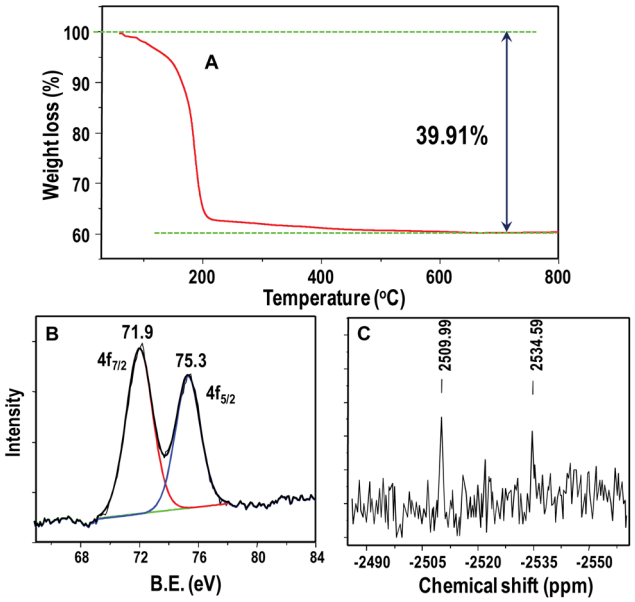

Fig. 3 TG analysis of the $Pt_{11}(BBS)_8$ cluster (A). Extended XPS (B) and ^{195}Pt NMR (C) of the Pt_{11} cluster. For NMR measurement K_2PtCl_6 was taken as the standard.

^{195}Pt NMR studies were conducted on the HPLC purified cluster to understand structural details about the cluster (Experimental details are presented in S1, ESI†). Fig. S15, ESI† shows the spectrum of the K_2PtCl_6 standard, which is used for this purpose in similar studies.[42] Note that ^{195}Pt is having only a natural abundance of 33.7% with a wide range of chemical shifts which cover about 15 000 ppm, ranging from +11 840 ppm ($[PtF_6]^{2-}$) to −3000 ppm (Pt(0) complexes). This makes it very difficult in studying such NMR unless one knows about the possible chemical shift for the peaks. It is difficult to extract information also because no such report about such clusters exists in the literature. K_2PtCl_6 was taken as the standard in our measurements which shows a line at 0.0008 ppm. The negative shift was seen (Fig. 3C) in the spectrum of the cluster as expected for a Pt(0) cluster.[43] Two peaks appearing at −2509 and −2534.5 ppm, respectively, (Fig. 3C) suggest the possibility of two distinct environments in the cluster. For the Au_{11} system, two kinds of distinct environments exist.[44] The intensity ratio of the peaks is 6 : 5 (taking the area of the peaks), which is distinctly different from 8 : 3, expected if 8 ligands are directly connected to the Pt atoms. The observed intensity ratio suggests that there are bridging ligands as in the case of gold clusters.

The purified cluster is stable for 10 days under ambient conditions (Fig. S16A, ESI†). Gradually it degrades to form thiolates. The cluster is compatible with many solvents (Fig. S16B, ESI†). Efforts are being made to crystallize the cluster.

In summary, undecaplatinum clusters were synthesized successfully through a solid state route. The crude cluster was purified using HPLC. It shows a blue luminescence with a quantum yield of 3×10^{-3}, comparable to that of gold clusters. The precise composition of $Pt_{11}(BBS)_8$ was determined from

MALDI MS and ESI MS analyses. Several other studies support the results. Atomically precise and soluble platinum clusters of this kind may be useful for homogeneous organic catalysis. Use of other ligands and adsorption on proper supports may enhance their stability.

We thank the Department of Science and Technology, Government of India for constantly supporting our research program on nanomaterials. I.C. and S.B thank IITM and R.G.B. thanks CSIR, Government of India for research fellowships. Thanks to M.S Boothraju for XPS analysis. We also thank Tata Institute of Fundamental Research (TIFR), India for ^{195}Pt NMR studies.

Notes and references

1 C. M. Aikens, *J. Phys. Chem. C*, 2008, **112**, 19797–19800.
2 T. P. Bigioni, R. L. Whetten and Ö. Dag, *J. Phys. Chem. B*, 2000, **104**, 6983–6986.
3 S. Link, A. Beeby, S. FitzGerald, M. A. El-Sayed, T. G. Schaaff and R. L. Whetten, *J. Phys. Chem. B*, 2002, **106**, 3410–3415.
4 K. Nobusada and T. Iwasa, *J. Phys. Chem. C*, 2007, **111**, 14279–14282.
5 G. Wang, T. Huang, R. W. Murray, L. Menard and R. G. Nuzzo, *J. Am. Chem. Soc.*, 2004, **127**, 812–813.
6 M. Zhu, C. M. Aikens, F. J. Hollander, G. C. Schatz and R. Jin, *J. Am. Chem. Soc.*, 2008, **130**, 5883–5885.
7 M. A. H. Muhammed and T. Pradeep, in *Advanced Fluorescence Reporters in Chemistry and Biology II*, ed. A. P. Demchenko, Springer, Berlin Heidelberg, 2010, vol. 9, ch. 11, pp. 333–353.
8 C.-A. J. Lin, T.-Y. Yang, C.-H. Lee, S. H. Huang, R. A. Sperling, M. Zanella, J. K. Li, J.-L. Shen, H.-H. Wang, H.-I. Yeh, W. J. Parak and W. H. Chang, *ACS Nano*, 2009, **3**, 395–401.
9 T. Chen, S. Xu, T. Zhao, L. Zhu, D. Wei, Y. Li, H. Zhang and C. Zhao, *ACS Appl. Mater. Interfaces*, 2012, **4**, 5766–5774.
10 Y. Kong, J. Chen, F. Gao, R. Brydson, B. Johnson, G. Heath, Y. Zhang, L. Wu and D. Zhou, *Nanoscale*, 2013, **5**, 1009–1017.
11 I. Chakraborty, T. Udayabhaskararao, G. K. Deepesh and T. Pradeep, *J. Mater. Chem. B*, 2013, **1**, 4059–4064.
12 I. Chakraborty, S. Bag, U. Landman and T. Pradeep, *J. Phys. Chem. Lett.*, 2013, **4**, 2769–2773.
13 A. Das, T. Li, K. Nobusada, C. Zeng, N. L. Rosi and R. Jin, *J. Am. Chem. Soc.*, 2013, **135**, 18264–18267.
14 M. W. Heaven, A. Dass, P. S. White, K. M. Holt and R. W. Murray, *J. Am. Chem. Soc.*, 2008, **130**, 3754–3755.
15 C. Zeng, H. Qian, T. Li, G. Li, N. L. Rosi, B. Yoon, R. N. Barnett, R. L. Whetten, U. Landman and R. Jin, *Angew. Chem., Int. Ed.*, 2012, **51**, 13114–13118.
16 H. Qian, W. T. Eckenhoff, Y. Zhu, T. Pintauer and R. Jin, *J. Am. Chem. Soc.*, 2010, **132**, 8280–8281.
17 Y. Pei, Y. Gao and X. C. Zeng, *J. Am. Chem. Soc.*, 2008, **130**, 7830–7832.
18 P. D. Jadzinsky, G. Calero, C. J. Ackerson, D. A. Bushnell and R. D. Kornberg, *Science*, 2007, **318**, 430–433.
19 T. Udaya Bhaskara Rao and T. Pradeep, *Angew. Chem., Int. Ed.*, 2010, **49**, 3925–3929.
20 T. U. B. Rao, B. Nataraju and T. Pradeep, *J. Am. Chem. Soc.*, 2010, **132**, 16304–16307.
21 J. Guo, S. Kumar, M. Bolan, A. Desireddy, T. P. Bigioni and W. P. Griffith, *Anal. Chem.*, 2012, **84**, 5304–5308.
22 K. M. Harkness, Y. Tang, A. Dass, J. Pan, N. Kothalawala, V. J. Reddy, D. E. Cliffel, B. Demeler, F. Stellacci, O. M. Bakr and J. A. McLean, *Nanoscale*, 2012, **4**, 4269–4274.
23 I. Chakraborty, W. Kurashige, K. Kanehira, L. Gell, H. Häkkinen, Y. Negishi and T. Pradeep, *J. Phys. Chem. Lett.*, 2013, **4**, 3351–3355.
24 I. Chakraborty, A. Govindarajan, J. Erusappan, A. Ghosh, T. Pradeep, B. Yoon, R. L. Whetten and U. Landman, *Nano Lett.*, 2012, **12**, 5861–5866.
25 H. Yang, J. Lei, B. Wu, Y. Wang, M. Zhou, A. Xia, L. Zheng and N. Zheng, *Chem. Commun.*, 2013, **49**, 300–302.
26 H. Yang, Y. Wang and N. Zheng, *Nanoscale*, 2013, **5**, 2674–2677.
27 A. Desireddy, B. E. Conn, J. Guo, B. Yoon, R. N. Barnett, B. M. Monahan, K. Kirschbaum, W. P. Griffith, R. L. Whetten, U. Landman and T. P. Bigioni, *Nature*, 2013, **501**, 399–402.
28 H. Yang, Y. Wang, H. Huang, L. Gell, L. Lehtovaara, S. Malola, H. Häkkinen and N. Zheng, *Nat. Commun.*, 2013, 4.
29 S.-I. Tanaka, J. Miyazaki, D. K. Tiwari, T. Jin and Y. Inouye, *Angew. Chem., Int. Ed.*, 2011, **50**, 431–435.
30 X. Huang, B. Li, L. Li, H. Zhang, I. Majeed, I. Hussain and B. Tan, *J. Phys. Chem. C*, 2012, **116**, 448–455.
31 X. Le Guével, V. Trouillet, C. Spies, G. Jung and M. Schneider, *J. Phys. Chem. C*, 2012, **116**, 6047–6051.
32 H. Kawasaki, H. Yamamoto, H. Fujimori, R. Arakawa, M. Inada and Y. Iwasaki, *Chem. Commun.*, 2010, **46**, 3759–3761.
33 P. N. Duchesne and P. Zhang, *Nanoscale*, 2012, **4**, 4199–4205.
34 S. M. Reilly, T. Krick and A. Dass, *J. Phys. Chem. C*, 2009, **114**, 741–745.
35 S. Wang, H. Yao, S. Sato and K. Kimura, *J. Am. Chem. Soc.*, 2004, **126**, 7438–7439.
36 S. Knoppe, A. C. Dharmaratne, E. Schreiner, A. Dass and T. Bürgi, *J. Am. Chem. Soc.*, 2010, **132**, 16783–16789.
37 H. Qian, Y. Zhu and R. Jin, *Proc. Natl. Acad. Sci.*, 2012, **109**, 696–700.
38 A. V. Sberegaeva, W.-G. Liu, R. J. Nielsen, W. A. Goddard and A. N. Vedernikov, *J. Am. Chem. Soc.*, 2014, **136**, 4761–4768.
39 H. Kang, *Acc. Chem. Res.*, 2005, **38**, 893–900.
40 G. H. Woehrle and J. E. Hutchison, *Inorg. Chem.*, 2005, **44**, 6149–6158.
41 G. H. Woehrle, M. G. Warner and J. E. Hutchison, *J. Phys. Chem. B*, 2002, **106**, 9979–9981.
42 M. Kirchmann, K. Eichele, F. M. Schappacher, R. Pöttgen and L. Wesemann, *Angew. Chem., Int. Ed.*, 2008, **47**, 963–966.
43 Y. Koie, S. Shinoda and Y. Saito, *J. Chem. Soc., Dalton Trans.*, 1981, 1082–1088, DOI: 10.1039/DT9810001082.
44 P. A. Bartlett, B. Bauer and S. J. Singer, *J. Am. Chem. Soc.*, 1978, **100**, 5085–5089.

